Journal of Food Measurement and Characterization
https://doi.org/10.1007/s11694-023-02011-6

ORIGINAL PAPER

Physical and antimicrobial performance of edible films based on oregano essential oil and tapioca starch emulsions

Paola Alzate[1,2,3] · Lía Gerschenson[1,2] · Giovanni Rojas[3] · Silvia Flores[1,2]

Received: 22 March 2023 / Accepted: 7 June 2023

Abstract

The development of environmentally friendly materials based on natural and biodegradable sources, such as starch, represents an interesting alternative to attend to the environmental problems caused by excess waste from petroleum-based packaging. The use of emulsions to obtain edible films is a novel strategy to be explored to determine how formulation and constitution affect film properties. In such context, gelatinized tapioca starch (TS) and oregano essential oil (OEO) were used to produce new active edible films using casting technique and their physical and antimicrobial properties were studied. Regarding the emulsion constitution, which was obtained employing an high-speed homogenizer, exposure to ultrasound (US) and surfactant Tween 80 (T80) content, had relevant effects on micro (0.2 to 105 µm) and nanometric (63 to 212 nm) size distributions of the TS particles and the OEO droplets. Exposure to US reduced (4.8–34 µm) and stabilized microparticles but promoted nanoparticle aggregation during storage, independently of T80 addition. T80 helped to stabilize coarse emulsions showing a Sauter diameter of 21.4 µm along storage. Films from coarse emulsions containing OEO and T80 were stiffer (stress at break: 1.8 MPa), less soluble in water (≈ 35%) and yellowish than films without T80. In addition, surfactant promoted a discontinuous microstructure of the film matrix. Both films containing OEO showed a good capacity to inhibit the growth of spoilage microorganisms (≈ 2.5–4 log cycles reductions). Due to their performance as physical and antimicrobial barriers, the films can be proposed as active packaging alternatives to stabilize and release natural preservatives to promote food preservation during storage and as a tool to support environmental sustainability.

Keywords Biopolymer matrix · Size distribution · Structure · Active packaging · Spoilage microorganisms · Food preservation

Introduction

Due to the numerous environmental problems caused by excess waste from petroleum-based packaging, researchers are focusing extensively on the development of environmental friendly materials using natural and biodegradable biopolymers [1, 2]. Starch is considered a promising candidate to obtain sustainable materials because it is biodegradable, renewable, and low-priced. Starch materials have advantages such as transparency and low permeability to oxygen and carbon dioxide [3]. Since starch has high availability and good extraction yield it can be used as a natural raw material to prepare edible films or coatings; specifically, tapioca starch (TS) films, have unique characteristics such as colorless, odorless, tasteless, nontoxic, and semi permeability to gases, lipids, flavor compounds. This starch is suitable for food packaging systems and can be used with the aim to minimize wastes of non-degradable materials [3, 4].

Additionally, active packaging can be obtained by the addition of bioactive compounds, such as antimicrobials, creating a functional packaging that could extend the shelf-life of foods [5–7]. According to recent studies, there has been a large interest in the application of polysaccharide-based edible coating

✉ Silvia Flores
sflores@di.fcen.uba.ar

1 Departamento de Industrias, Facultad de Ciencias Exactas y Naturales, Universidad de Buenos Aires, Intendente Guiraldes 2620, 1428 Ciudad Autónoma de Buenos Aires, Argentina

2 Instituto de Tecnología de Alimentos y Procesos Químicos (ITAPROQ), CONICET - Universidad de Buenos Aires, Buenos Aires, Argentina

3 Departamento de Ciencias Químicas, Facultad de Ciencias Naturales, Universidad ICESI, Cali, Colombia

Published online: 14 June 2023

with essential oils (EOs) due to their strong antioxidant and antimicrobial characteristics [8].

Micro/nano oil-in-water (O/W) emulsions are efficient vehicles for hydrophobic compounds since, after the emulsification and dehydration process, lipophilic bioactive molecules can be incorporated into the film matrix. Usually, the use of O/W emulsions increases dispersibility and protection against oxidation or other interactions with food ingredients [9]. Using of ultrasound (US) for fine emulsion's formation has been recommended since smaller droplet sizes can be obtained to improve encapsulation and retention of the active agents [10]. Usually, whey protein, starches or maltodextrins are used as stabilizers of emulsions in the food industry [11]. Additionally, surfactants can be added to stabilize the O/W interface. For example, polyoxyethylene(20)sorbitan monooleate, Tween 80® (T80), is widely used as a nonionic emulsifier in diverse formulations [12]. The use of emulsions to obtain new materials is an alternative that must be explored to determine how formulation and constitution process affect film properties [13].

Plant-based EOs are natural additives often used to protect food against oxidation and microbial growth. Most EOs are considered generally recognized as safe (GRAS) according to the USFDA and can be used as natural ingredients to improve the mechanical and barrier properties of films. They can also promote beneficial properties, such as antioxidant and/or antimicrobial activity. For example, oregano essential oil (OEO) is a good alternative as a food preservative, mainly because it contains high levels of carvacrol and thymol [14].

Although there are many reports describing the properties of films containing EOs, it is scarce research analyzing the effect of the oil phase structure and, at the same time, the aqueous phase formulation with the addition of starch as a thickening agent and surfactant, on the characteristics and functionalities of the resulting films which could be considered for a potential food packaging material.

The objectives of the research were to present a methodology for obtaining O/W emulsions from TS solutions containing OEO and to analyze the effects of the T80 addition and exposure to US on the structure and stability of the emulsions. In addition, selected emulsions were studied to allow the production of edible films. The physical, chemical, and mechanical characteristics of films were investigated to determine the relationships between the emulsion structure and the properties of the final film material, especially their antimicrobial capabilities against some spoilage microorganisms.

Materials and methods

Preparation of emulsions

TS (Bernesa S.A., Argentina), OEO (Euma S.A.I.C.I.yF., Argentina) and T80 (Alkest, Manuchar, Mexico) were used as received. Starch aqueous suspensions (3.0% w/w) were prepared and heated at approximately 85 °C until gelatinization. After cooling to room temperature, the slurries were added with OEO (0.75% w/w). As shown in Table 1, 0.25% w/w of T80 was added to some samples. All samples were coarse homogenized at high-speed using a device Ultra Turrax® (IKA, Germany) at 13,500 RPM for 2 min. When necessary, some suspensions were exposed to US (Table 1) with a frequency of 20 kHz and 750 W (Sonics VCX-750, USA) using 70% amplitude for 2 min. All emulsions were hermetically sealed and stored at 25 °C. For comparison proposes, three additional control systems were produced: COT80, CTS and CTSUS (Table 1).

Characterization of emulsions

Size distributions and Z-potential of emulsions

The micrometric size distributions of emulsions were determined by static light scattering (SLS) while the nanometric Z-average (the intensity-weighted mean hydrodynamic size of particles) and Z-potential (ζ-pot, the electric potential difference between the dispersion medium and the stationary layer of fluid attached to the dispersed particle) were characterized by dynamic light scattering (DLS), both at 25 °C. Experimental details are described in supplementary information file, SI1.

Obtaining films from emulsions

Selected emulsions were used for film casting [14] previously added with glycerol (1.0% w/w) as a plasticizer. Aliquots of systems (12 g) were placed on silicone plates and dried for 18 h at 40 °C in an oven with air convection to achieve film constitution. Before characterization, films were separated from the plates and stabilized in an atmosphere of 57% relative humidity for 15 days at 25 °C.

Physicochemical characterization of films

Films were characterized by determination of their color, opacity, mechanical properties (tensile test), water vapor permeability (WVP), solubility in water (S) and microstructure. Experimental details are described in SI1.

Chemical structure and interactions

Fourier transform infrared (FTIR) spectra were obtained in the range of 400 to 4000 cm^{-1}. The spectra were recorded using an Attenuated Total Reflectance (ATR) device and software Spectrum V5.3.1 (Perkin Elmer, Inc., Massachusetts, USA).

Table 1 Micrometric range of size distribution of emulsified systems

System	Conditions[†]	Time (days)	d(0.1) (μm)	d(0.5) (μm)	d(0.9) (μm)	Span	D[3.2] (μm)
S1	TS, OEO With US	0	6.41 ± 0.09	10.1 ± 0.2^{a}	15.6 ± 0.5^{b}	0.91 ± 0.4	9.4 ± 0.1
		5	5.8 ± 0.1	9.8 ± 0.1^{a}	15.9 ± 0.4^{b}	1.03 ± 0.05	9.0 ± 0.1
		20	4.8 ± 0.1	9.9 ± 0.8^{a}	22 ± 5	1.7 ± 0.4	8.6 ± 0.5
S2	TS, OEO No US	0	5.55 ± 0.03	15.5 ± 0.5^{C}	57 ± 5^{c}	3.3 ± 0.3	11.7 ± 0.2
		5	6.56 ± 0.07	17.9 ± 0.7^{D}	67 ± 7^{c}	3.4 ± 0.4	13.7 ± 0.3^{d}
		20	6.2 ± 0.2	17 ± 1^{E}	105 ± 20	6.1 ± 0.8	13.6 ± 0.9^{d}
S3	TS, OEO, T80 With US	0	9 ± 2^{e}	16 ± 4$^{f, C}$	28 ± 8$^{h, F}$	1.2 ± 0.1	14 ± 3$^{i, G}$
		5	11 ± 2	20 ± 4$^{g, D}$	34 ± 7^{h}	1.1 ± 0.1	18 ± 3
		20	8.31 ± 0.05^{e}	17.13 ± 0.07$^{f, g, E}$	30.8 ± 0.2^{h}	1.316 ± 0.005	14.25 ± 0.07^{i}
S4	TS, OEO, T80 No US	0	0.201 ± 0.003^{A}	4.8 ± 0.2^{B}	34.8 ± 0.9^{F}	7.2 ± 0.2	0.61 ± 0.01
		5	12.24 ± 0.04	25 ± 2	49 ± 1	1.43 ± 0.08	21.4 ± 0.2^{j}
		20	13.4 ± 0.3	23.4 ± 0.3	40 ± 1	1.15 ± 0.06	21.4 ± 0.2^{j}
COT80	OEO, T80 No US	0	0.151 ± 0.003^{A}	0.29 ± 0.02	0.9 ± 0.2	2.7 ± 0.5	0.27 ± 0.01
CTS	TS No US	0	4.9 ± 0.3	34 ± 2	112 ± 23	3.1 ± 0.6	14.5 ± 0.7^{G}
CTSUS	TS With US	0	2.7 ± 0.2	5.8 ± 0.5^{B}	27 ± 4^{F}	4.3 ± 0.8	5.2 ± 0.4

TS tapioca starch, *OEO* oregano essential oil, *T80* Tween 80, *US* ultrasound, + presence and − absence

Average values and standard deviations are reported

Same lowercase letter indicates no significant differences during storage for the same size parameter and conditions (α = 0.05). Same capital letter indicates no significant differences for the same size parameter and storage time, but different conditions (α = 0.05)

[†]Condition column summarizes the experimental conditions used for preparing systems from S1 to S4 and the controls (COT80, CTS and CTSUS)

Antimicrobial capacity of films

Antimicrobial capacity was studied by exposing films to *Pseudomonas aeruginosa, Lactobacillus plantarum* and *Zygosaccharomyces bailii* contamination [15]. Muller Hinton, De Man-Rogosa-Sharpe and Sabouraud agars (Biokar, France) were used for each microorganism, respectively. A model food with a high-water activity (~ 0.98) was formulated from the corresponding agars by dextrose (Anedra, Argentina) addition. In addition, the pH of Sabouraud agar was lowered to 4.5 by adding a 50% (w/w) solution of sterile citric acid (Anedra, Argentina). Disks of 1 cm diameter from samples and control system (CTS) were cut aseptically, weighed, and placed on the surfaces of plates containing the appropriate agars for each microorganism to be tested. Then, 10 μL of inoculum of 10^6 CFU/mL of *P. aeruginosa* or *L. plantarum* and 10^5 CFU/mL of *Z. bailii* were seeded onto the film discs, and the systems were incubated at 25 °C. At selected times, two discs from each microorganism were sampled and each one was suspended in 1 mL of sterile peptone water (Biokar, France) contained in a glass tube. The microorganisms were re-suspended by shaking the tube for 2 min at 2500 RPM with a vortex (Ika., USA). A series of dilutions were then prepared in peptone water for cell counting (CFU/g film). Bacteria were enumerated by deep seeding on the corresponding agars, followed by incubation at 37 °C for 48–72 h. The study of the yeast population was performed by plating on Sabouraud agar and incubation at 25 °C for 5 days before counting.

Statistical analysis

All determinations were carried out, at least, in duplicate. In most cases, there were performed more than three independent replicates. Results are reported based on their averages and standard deviations. Significant differences between the systems were established through ANOVA (α = 0.05). Statgraphics Centurion XV 2.15.06 (2007) software was used for statistical analysis of the data.

Results and discussion

Particle size distribution and ζ-pot of emulsions

Micrometric size distribution

Table 1 shows the SLS results of the micrometric range of size distribution for all emulsions. At day zero, exposure to US produced, in general, smaller particles with lower

dispersion and span values (S1 vs S2). The T80 addition to the sonicated emulsion (S3) promoted an increase in particle sizes but with a similar span (S3 vs S1). However, T80 generally assisted to reduce the particle diameters in coarse emulsion (S4), even though a higher value of span was observed (S4 vs S2).

Regarding the stability of emulsions along storage, it was observed that the diameters corresponding to 10, 50, or 90% of the cumulative population, d(0.1), d(0.5) and d(0.9) values ranged from 6.4 to 16 µm for S1 being, in general, smaller than S2 which showed values from 5.6 to 57 µm, when particles were freshly prepared. After 20 days of storage, the sizes tended to increase in S1 and S2 emulsions. The same tendency was observed when comparing S3 to S4. These results confirmed that the cavitation energy incorporated through US exposure promotes mechanical size reduction of particles in O/W emulsions containing EOs and gelatinized starch [16–18]. In addition, there was little dispersion when US was applied, since S1 and S3 systems showed span values around 1.2 along storage. In general, particles exposed to US only (S1) showed smaller variations in terms of Sauter diameter, D[2,3], (the diameter of a sphere having the same volume/surface ratio as the particle of interest) than S2 during 20 days. However, in the same period, span values were almost doubled for S2, probably due to the high variability in d(0.9) at the end of storage as a consequence of a possible aggregation of particles.

The micrometric parameters, d and D[2,3] at 5 and 20 days of storage, for samples containing T80 (S3 and S4), showed larger particles compared to emulsions without T80 (S1 and S2). Table 1 shows that S3 had a fluctuant character during storage while the sizes of S4 increased around 5 times after 5 days, after which size distribution did not change significantly ($p > 0.05$). In addition, span was highly reduced after 5 days, suggesting stabilization of this emulsion.

Nanometric size distribution

Table 2 shows the results obtained from DLS analysis. Particles Z-averages ranged from 63 to 212 nm, and the highest PDI was 0.40. These size values are desired since emulsions exhibiting average particle size between 10 and 200 nm, having various applications in delivery of functional compounds which are hydrophobic in nature [17]. For S1 to S4 emulsions, ζ-pot showed negative values, which is consistent with the formation of particles with low dispersion bearing a negative charge on the particle surface. For freshly prepared emulsions, S1 and S4 showed the highest electro-kinetic potential, − 19 and − 39 mV, respectively, indicating that those preparations could form stable systems. Usually, emulsions with ζ-pot modulus in the range of 40

Table 2 Nanometric Z-average and ζ-pot of emulsified systems

System	Conditions[†]	Time (days)	Z-average (nm)	PDI	ζ-pot average (mV)
S1	TS, OEO With US	0	85 ± 2^{a}	0.19 ± 0.01^{b}	-19 ± 2
		5	83 ± 1^{a}	0.18 ± 0.01^{b}	-1.1 ± 0.9^{D}
		20	163 ± 3	0.40 ± 0.02^{C}	-6.5 ± 0.9
S2	TS, OEO No US	0	212 ± 6	0.4 ± 0.1^{B}	-11 ± 1
		5	72 ± 1	0.29 ± 0.01^{c}	-5.0 ± 0.5
		20	144 ± 7	0.3 ± 0.01^{c}	-0.7 ± 0.5
S3	TS, OEO, T80 With US	0	108 ± 3^{A}	$0.29 \pm 0.03^{d, B}$	-4.2 ± 0.6
		5	77.4 ± 0.8	0.21 ± 0.01	-3 ± 1^{D}
		20	170 ± 2	$0.36 \pm 0.05^{d, C}$	-7 ± 1
S4	TS, OEO, T80 No US	0	169 ± 4	0.35 ± 0.04^{B}	-39 ± 2
		5	63 ± 4	0.27 ± 0.01^{e}	-33 ± 3
		20	95 ± 1	0.25 ± 0.01^{e}	-2.3 ± 0.6
COT80	OEO, T80 No US	0	257 ± 5	0.40 ± 0.02^{B}	-6 ± 2
CTS	TS No US	0	N.D	N.D	N.D
CTSUS	TS With US	0	105 ± 1^{A}	0.36 ± 0.02^{B}	-1.1 ± 0.1

N.D. not detectable

Average values and standard deviations are reported. Same lowercase letter indicates no significant differences during storage for the same parameter and conditions ($\alpha = 0.05$). Same capital letter indicates no significant differences for the same parameter and storage time, but different components ($\alpha = 0.05$)

[†]Condition column summarizes the experimental conditions used for preparing systems from S1 to S4 and the controls (COT80, CTS and CTSUS)

to 60 mV are considered as moderately stable and avoid aggregation or flocculation of particles, since electrostatic repulsions are high enough to keep them apart [10]. However, the surface charge of all emulsions normally decreases (absolute magnitude) over time, allowing some aggregation [18], as can be observed in Table 2 for each system after 5 and 20 days of storage.

Although exposure to US reduced the particle size, an aggregation phenomenon was usually observed after long periods of storage. Freshly prepared S1 and S3 emulsions showed the lowest Z-average values. After 20 days, these particles showed an enlargement of 34% and 57%, respectively. Possibly, the US reduced the aqueous phase viscosity due to particle size reduction, promoting faster aggregation of the nanometric fraction. The aggregation did not occur simultaneously in all particles, increasing the PDI in the both S1 and S3 systems. On the other hand, not sonicated emulsions, S2 and S4, were initially larger than those exposed to the US but then over time, they yielded the smallest nanometric particles at the end of storage, with S4 better than S2 in terms of ζ-pot. Hashtjin and Abbasi [19] also observed a downward trend in the size of orange EO drops in a nanoemulsion within the first 4 weeks followed by an increase in the Z-average, probably because of the coalescence and Ostwald ripening. The authors associated such phenomena with a gradual reduction in the kinetic energy barrier in this kind of emulsion at room temperature that delays reaching a kinetic equilibrium state, being this process modulated by oil–water interfacial tension.

To better understand the effects of the presence or absence of TS or OEO and T80 on the size and composition of micro and nanoparticles, three control systems COT80, CTS and CTSUS were analyzed (Tables 1 and 2). Particularly, Fig. 1 shows the SLS and DLS size distributions of S4 and control systems. Emulsion S4 clearly showed a bimodal distribution: a submicronic population and larger particles between 4.8 and 34.8 µm (Fig. 1a). Because it was also necessary to study the influence of TS on the formation of particles, COT80 was prepared using the same conditions as S4, but without TS. The COT80 particles showed a monomodal distribution mainly in the range of 0.15 to 0.9 µm with a small population in the range of 1 to 100 µm (Fig. 1b). The results verify that the presence of TS during formation of coarse emulsion contributes mainly to their micrometric fraction. To observe the structure of COT80 and S4 emulsions, optical microscopy images are provided in SI2 file. To discuss the contribution of TS, along with the absence of OEO and T80, CTS system was elaborated with gelatinized TS and

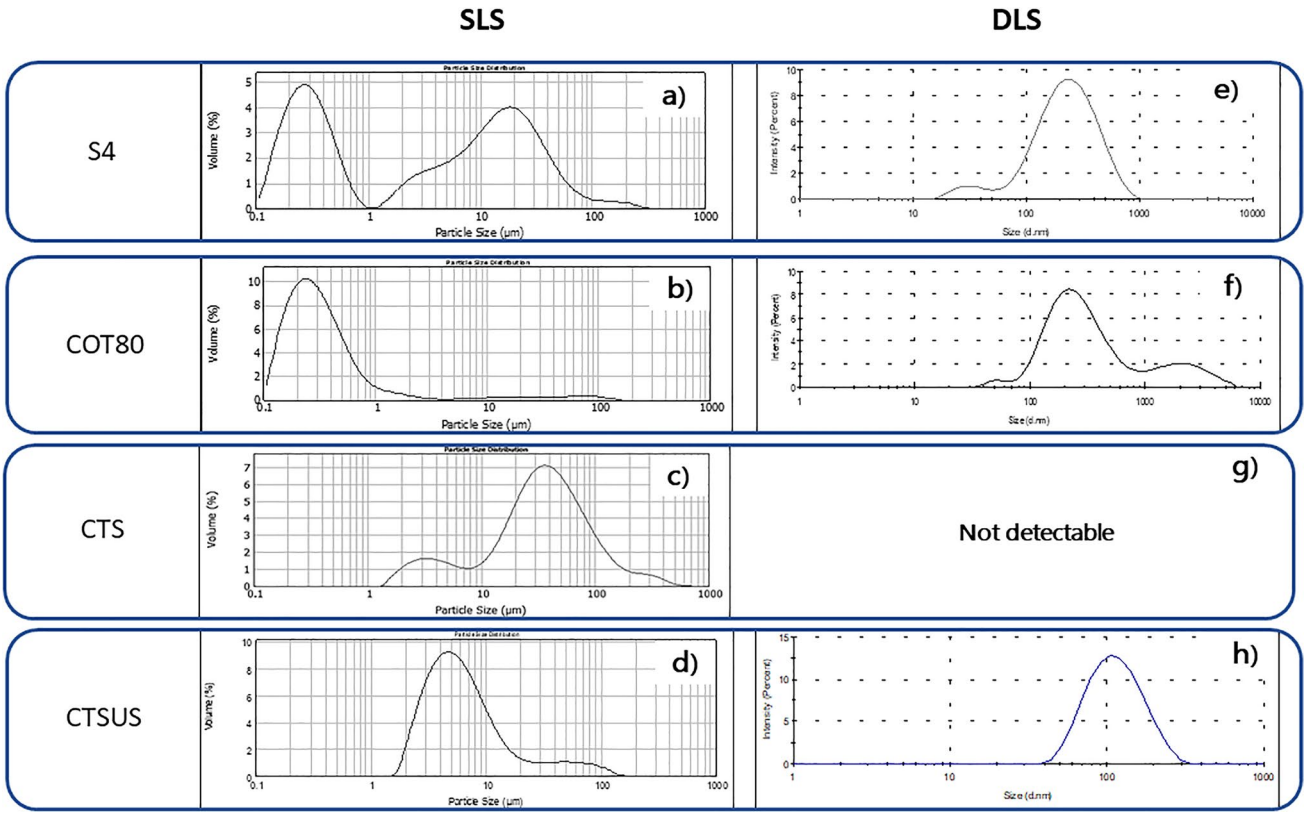

Fig. 1 Size distributions. Left column shows SLS results; right column shows DLS results. Top line (**a**) and (**e**) show S4. Second line (**b**) and (**f**) show COT80. Third line (**c**) and (**g**) show CTS. Bottom line (**c**) corresponds to CTSUS

only processed by high-speed homogenization. The CTS system formed larger microparticles than S4 with a bimodal profile (Fig. 1c, Table 1). When gelatinized TS was additionally exposed to US (CTSUS), as expected, particles were, in general, significantly ($p < 0.05$) smaller than those of CTS and S3 but with higher span value (Fig. 1d, Table 1).

Regarding the nanometric fractions, COT80 showed a bimodal population with a Z-average of 257 ± 5 nm, in agreement with SDS profile (Fig. 1b and f) and ζ-pot of -6 ± 2 mV (Table 2). Additionally, Table 2 and Fig. 1e, show that the Z-average of S4 was smaller than that of COT80. Xu et al. [20] reported that starch chains could act as an amorphous and flexible emulsifier that is placed in the interface of the O/W layers, helping to stabilize the oil droplets by reduction of interfacial tension. In addition, it was previously stated that hydrocolloid solutions, such as gelatinized starch, contribute to stabilization of emulsions by providing a viscous aqueous phase where diffusion of the disperse phase becomes slow. Silva et al. [10] obtained annatto seed oil emulsions stabilized by addition of modified starches (ratio oil:biopolymer 1:4 w/w), where the adsorption of the macromolecules on the surface of the oil drop was the predominant mechanism, together with changes in the viscosity of the overall system. It was also observed that CTS particles were not suitable for DLS measurements (Fig. 1g, Table 2), suggesting that TS without US application mainly contribute to micrometric fraction. Contrarily, CTSUS displayed a monomodal size distribution around 100 nm (Table 2), revealing that sonicated TS also constituted nanoparticles [18], in agreement with previous research [21]. Such trend could be observed for CTSUS particles in comparison to CTS (Table 2). In addition, it can be noticed that the presence of OEO/T80 and TS (S4) contributed to produce the smallest particles with narrow distribution in coarse emulsions (Table 2); in other words small particles with fewer aggregations.

In summary, regarding S1 to S4 emulsions, it can be concluded that US exposure allowed the formation of smaller and more homogeneous distribution of microparticles but promote aggregation in nanoparticles, independently of T80 addition, along storage. The role of T80 for both nanometric and micrometric dimensions is closely dependent on the US, producing larger particles when both are applied, as shown in Tables 1 and 2 for S3 in comparison with S1, probably because of the reduced viscosity of aqueous phase when the US was applied. On the other hand, emulsions that were not exposed to the US, i.e., S2 and S4, were quite stable after 5 days of storage (Table 1) and rendered smaller nanoparticles, which is necessary for real shelf applications. This nano-fraction might be constituted mainly by OEO, which should be optimized for antimicrobial performance. In addition, S2 and S4 were prepared using a simpler and cheaper emulsification process. According to these results, samples from S2 and S4 were selected for casting active edible films to protect, encapsulate, and deliver OEO.

Physicochemical characterization of films

Since particles from emulsions S2 and S4 showed convenient behavior in terms of nanometric Z-average, ζ-pot, dispersity, and long-term stability they were used for casting films. Table 3 summarizes the properties of the obtained films from S2 and S4 emulsions**.** It could be observed that both films showed similar L* and a* color parameters, and opacity ($p > 0.05$), where L* is related to the perceptual lightness, a* and b* are for the colors red, green, blue, and yellow. On the other hand, the yellowness index (YI) for S2 was 29% larger ($p < 0.05$) than that for S4. The same trend was observed for b*. Saberi et al. [22], observed the same tendency in films prepared with pea starch containing Tween 20. The authors indicated that the surfactant molecules modified the emulsion structure, affecting the light dispersion, and thus decreasing the yellow color.

Additionally, the mechanical properties of films are reported in Table 3 and Fig. 2. The profile indicates a ductile behavior with an initial rapid increase of stress along with increasing deformation (solid response), followed by a plastic response, where the stress slightly changed until its rupture. It was observed that system S4 showed higher ($p < 0.05$) elastic modulus (EM) and stress at break (σ_r) with a lower deformation (ε_r) than S2. Ortega-Toro et al. [23] observed low deformability and high resistance to tensile forces in corn starch-based films added with surfactant. The authors attributed those results to the formation of starch-surfactant complexes that rendered crystalline aggregates. In addition, S4 films showed a 34.9% reduction in moisture

Table 3 CIELAB color space parameters, mechanical properties, moisture content, solubility in water and water vapor permeability of films obtained from S2 and S4 emulsions

	S2	S4
L*	89.8 ± 0.3^{a}	89.5 ± 0.2^{a}
a*	-1.29 ± 0.05^{b}	-1.31 ± 0.02^{b}
b*	4.7 ± 0.3	4.1 ± 0.2
Yellowness Index	8.5 ± 0.6	6.6 ± 0.4
Opacity	44.6 ± 0.5^{c}	44.1 ± 0.3^{c}
EM (MPa)	13 ± 1	41 ± 3
σ_r (MPa)	0.89 ± 0.03	1.8 ± 0.2
ε_r (%)	93 ± 5	71 ± 7
Moisture (% d.b.)	33 ± 2	26 ± 3
S (%)	46 ± 2	34.9 ± 0.4
WVP × 10^9 (g/Pa m s)	1.41 ± 0.03^{d}	1.1 ± 0.1^{d}

Average value and standard deviation are reported. Same lowercase letter indicates no significant differences ($\alpha = 0.05$)

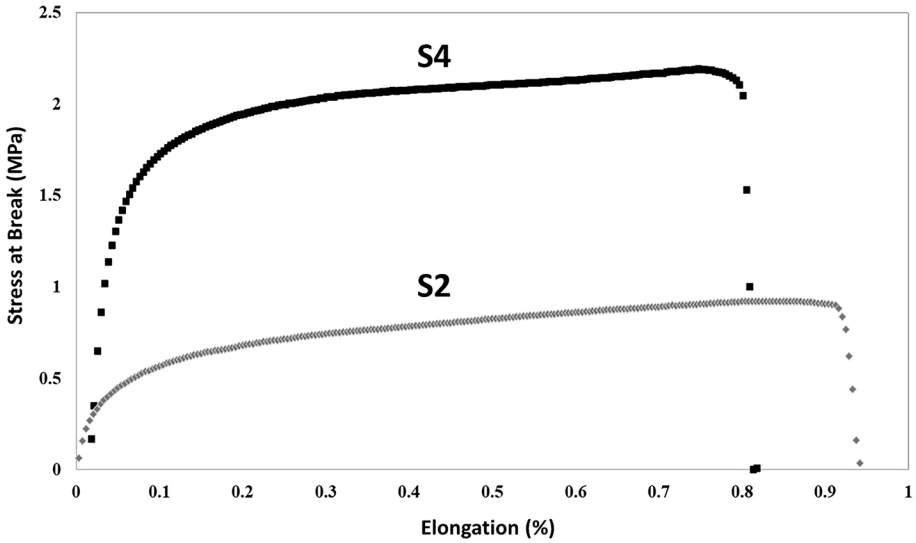

Fig. 2 Tensile test curves of starch films obtained from the S2 (without T80 and without US) and S4 (with T80 and without US) systems

content compared to S2 ($p < 0.05$) (Table 3), which could contribute to increasing EM and σ_r values.

Table 3 also shows that S of S4 was 46% lower than S2. Such results are expected, because the formation of an insoluble complex between starch and a surfactant reduces solubility, as observed by Santacruz et al. [24]. Solubility of materials is an important property that can help determine their applicability in food packaging. Thus, materials with high solubility can be used in food products with low moisture content, while materials with low solubility are useful even for food products with high moisture content [25, 26]. A similar tendency to lower values of WVP ($1.1 \pm 0.1 \times 10^{-9}$ g/Pa m s) for S4 in comparison to S2 ($1.41 \pm 0.03 \times 10^{-9}$ g/Pa m s) was observed, which agrees with the data reported previously [27], where the presence of T80 reduced the WVP in corn starch films. The hydrophilic groups of the surfactant decrease the film affinity towards water by blocking the number of available polar groups in the starch, and the non-polar groups in the surfactant repel water. The WVP results reported in Table 3 are consistent with data reported for starch-based edible films containing EOs components [14].

Microstructure of films

The microstructure of the film obtained is mostly determined by the structural arrangements of the film components, and this greatly affects the physical, mechanical, optical, and barrier properties of the films developed [26]. Figure 3 shows the morphology of the film surfaces and their cross-sections. The CTS film showed a rough and continuous surface with aggregates formed by TS (pointed out by arrows in Fig. 3a). The cross-section of CTS (Fig. 3b) displayed a dense and compact structure, consistent with an amorphous starch-based material, which rendered a soft and flexible film. The surface of S2 film was smoother in comparison with CTS, as shown in Fig. 3c. Some authors described that the non-polar liquid state of oils expands the droplets on the film surface after drying and fills the irregularities of the film matrix surface promoting formation of a single, smoother phase [28]. Figure 3d confirms that the S2 film cross-section is uniform and does not exhibit delamination or pores. Figure 3e shows the S4 surface with noticeable phase separation, marked by arrows. The presence of the T80 promoted agglomeration during the film casting process, yielding a discontinuous morphology. The formation of microdomains was promoted by the presence of T80, suggesting a partial integration of the surfactant in the starch matrix [23]. Figure 3f shows an uneven structure in the S4 cross-section. The presence of the emulsifier was necessary to stabilize the O/W emulsions; however, film dehydration affected T80 distribution promoting formation of micropores (Fig. 3f). According to Song et al. [29], the T80 incorporation into corn starch films containing lemon EO, critically affected the microstructure observing globules with rough surfaces due to liquid surfactant migration during drying, ultimately promoting phase separation and formation of micropores. It can be concluded that the specific interactions of surfactant with starch molecules and drying process modulated the distribution of T80 along the film matrix.

Chemical structure and interactions of films

Infrared analysis of the films provides information about the interactions of the individual compounds and the matrix. While Fig. 4a shows the IR spectra from films S2, S4 and the control system CTS, Fig. 4b shows the IR spectra of the individual components: T80, OEO, and pure carvacrol, as the main phenol in the OEO. The FTIR spectra of CTS, S2 and S4 showed typical patterns of starch materials. A

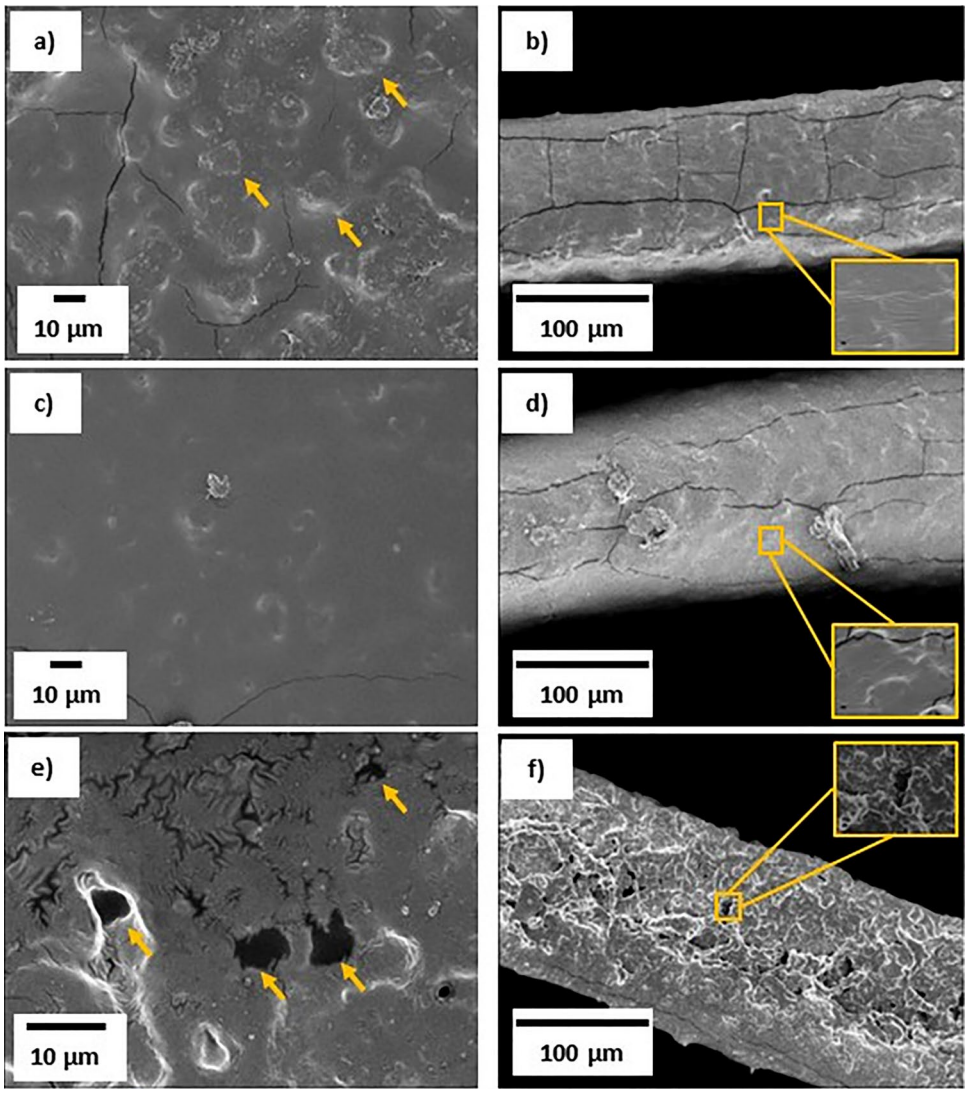

Fig. 3 SEM micrographs for **a** CTS surface, **b** CTS cross-section, **c** S2 surface, **d** S2 cross-section, **e** S4 surface and **f** S4 cross-section. Arrows point to starch and T80 aggregates

detailed description of main spectral bands is provided in SI2. An important broad band around 3290 cm^{-1} relates to the stretching of the O–H groups, which normally interact via intra- and intermolecular hydrogen bonds. The O–H stretch shifts to lower wavenumber in the following order: CTS > S2 > S4. According to Cao & Song [30], such displacement may be associated with new and strong hydrogen bonds arising among functional groups of components, i.e., starch, OEO and T80. The results suggest that additives promote interactions and consequently changes in molecular organization that also can improve film properties, such as solubility or mechanical resistance [31]. From Fig. 4b, it can be observed that the vibrations from carvacrol defined the IR profile of OEO, which is expected since carvacrol is one of the major components, along with thymol [28]. It is evident that the addition of OEO and T80 to film formulation did not alter the FTIR pattern of the S2 and S4 films. Probably, the concentrations of such additives were small and undetected by IR. Additionally, it can be concluded that no new covalent bonds were formed; instead, weak physical interactions were developed among components.

Antimicrobial capacity of the films

Since the main application of the produced films may be in the food packaging business, it is interesting to determine if OEO helps to extend food life. Figure 5 shows how the films S2, S4 and the control CTS behave when they are exposed to *P. aeruginosa*, *Zygosaccharomyces bailii* and *Lactiplantibacillus plantarum*. As expected, the control system CTS, which does not contain OEO, allowed growth of both bacteria, in 2.5 to 3 Log cycles, and yeast in 4 Log cycles after 72 h. Figure 5a shows that S2 and S4 reduced the growth of *P. aeruginosa* by 1 and 2 orders, respectively, after 72 h of storage, showing populations 3 and 4 orders lower than CTS. Regarding *L. plantarum*,

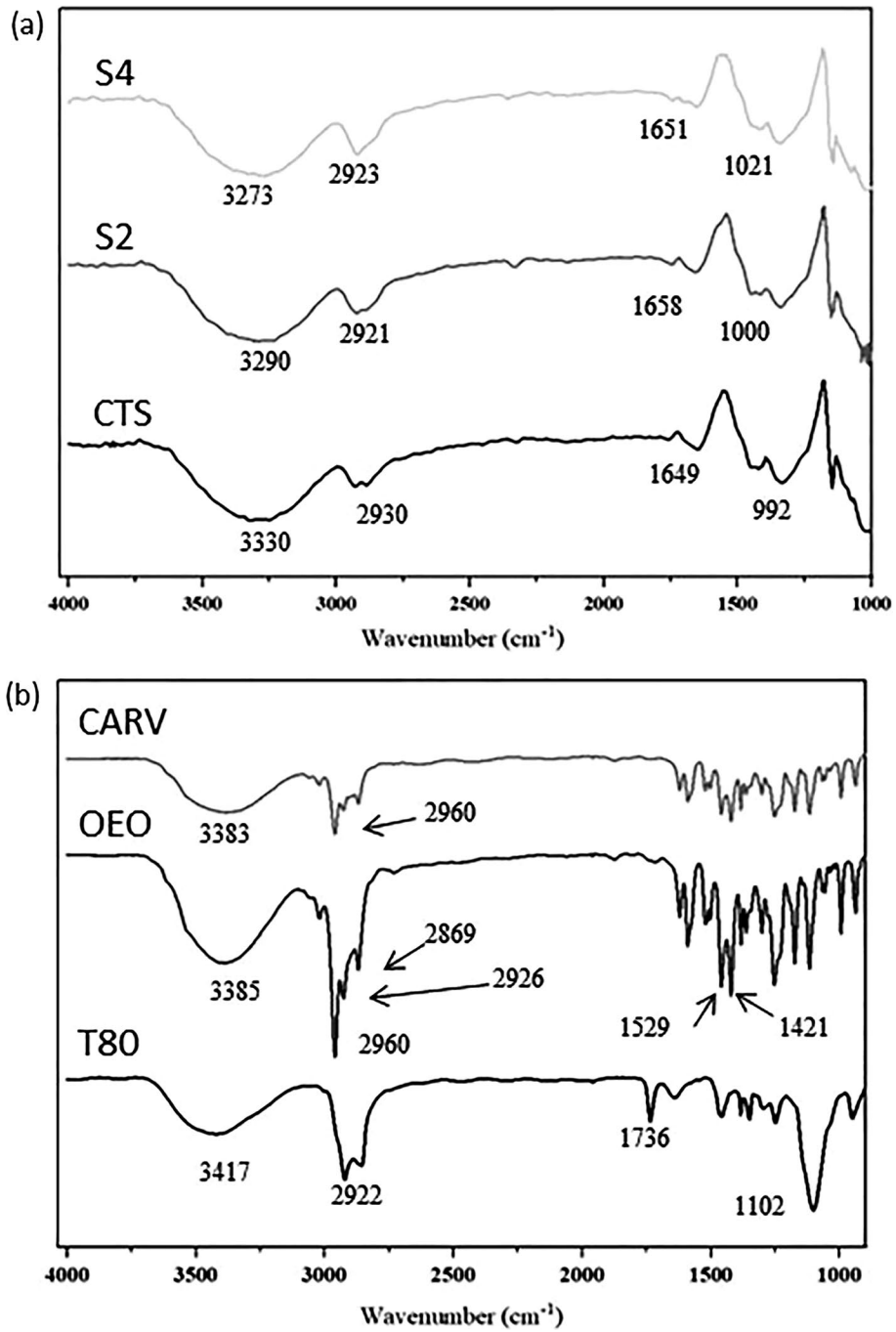

Fig. 4 FTIR spectra for **a** CTS, S2 and S4. **b** Carvacrol (CARV), oregano essential oil (OEO) and Tween 80 (T80)

neither S2 nor S4 films allowed bacterial development, reaching a lower cell count by 2.5 orders in comparison with CTS at the end of storage (Fig. 5c). Contrarily, yeast inoculated on the surfaces of films with OEO grew more slowly than yeast on CTS by 1.5 and 3 orders of magnitude higher than S2 and S4 after 72 h, respectively (Fig. 5b). In general, the results indicated that the presence of OEO in the films promoted an antimicrobial action, which was improved by the addition of T80 to the S4 film. Some authors highlight the antimicrobial activity of carvacrol and thymol, major components of oregano oil, since these constituents can disrupt the cell membrane by attacking its phospholipid bilayer and damaging enzyme systems, being effective antimicrobial substances that can be used in the formulation of biodegradable films [8]. Nielsen et al. [32] studied the effect of T80 on several strains and observed that its addition to the medium decreased the development of *L. monocytogenes* and *P. fluorescens*. The authors concluded that surfactant could affect the availability of nutrients in diverse ways, for example, by increasing the

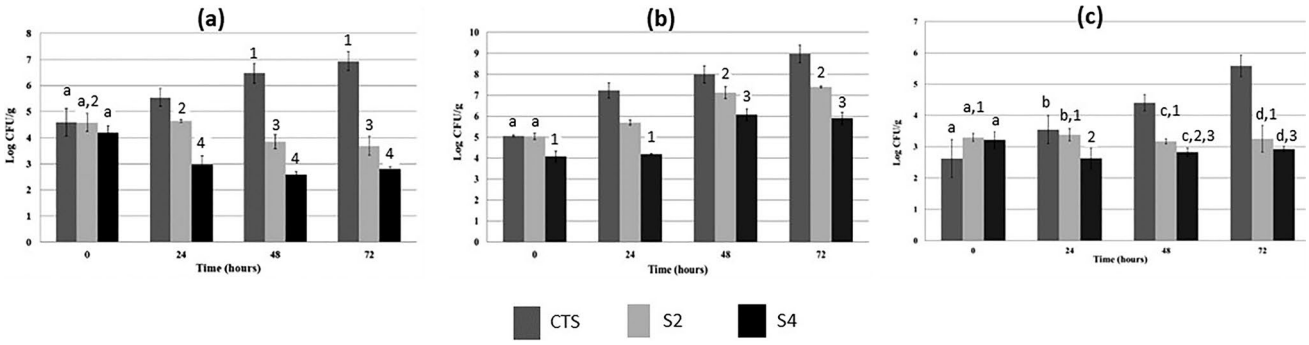

Fig. 5 Antimicrobial barrier capacity test of films S2, S4 and CTS against **a** *P. aeruginosa*, **b** *Z. bailii* and **c** *L. plantarum*. Average values and standard deviations are reported. Same lowercase letter indicates no significant differences between systems, same numeral indicates no significant differences across time for each system ($\alpha = 0.05$)

permeability of the membranes when it is present above a critical concentration. As was previously discussed, S4 emulsion containing T80 had the smallest size of nanoparticles that could be also improved the film antimicrobial action.

Conclusions

A series of materials with diverse chemical and physical properties based on TS were prepared. They demonstrated that it is possible to obtain edible films from emulsified systems of TS containing OEO as antimicrobial agent. Formation of emulsions showed that both OEO droplets and TS particles contributed to micro and nanometric size distributions. The TS enriched phase modulated the presence of micrometric particles in coarse emulsions. The OEO phase contributed primarily to the nanometric fraction of particles. Exposure to US was the factor with major effect on the characteristics of emulsions, by reducing and stabilizing microparticles but promoting nanoparticle aggregation after lengthy storage (20 days).

Starch based films containing OEO and T80, which were obtained from coarse emulsions, showed increased mechanical properties, with lower solubility and lower yellowish color, mainly due to the physical interactions among all components. However, T80 promoted an aggregated and discontinuous film microstructure, which limits the use for film casting. More importantly, all films containing OEO showed good capacity to inhibit spoilage microorganisms.

Therefore, the developed films are promising candidates to be used as edible and biodegradable active packaging materials that support antimicrobials and contribute to optimal food preservation, also contributing to environmental sustainability, which is a recent and innovative area in which further research is needed.

Supplementary Information The online version contains supplementary material available at https://doi.org/10.1007/s11694-023-02011-6.

Acknowledgements This study was financially supported by Universidad de Buenos Aires (UBACyT 20020170100092BA 2018–2022), Agencia Nacional de Promoción Científica y Tecnológica (PICT 2019-1842).

Author contributions PA performed the experiments and analyzed data, wrote the main manuscript text and prepared figures. LG contributed with conceptualization and resources. GR reviewed and edited the manuscript and contributed with resources. SF planned the investigation and methodology, elaborated conceptualization, contributed resources, analyzed data, wrote the main manuscript text, supervised the project, contributed with resources and funding and wrote the original draft, reviewed and edited the manuscript.

Data availability Data will be made available on request.

Declarations

Competing interests None of the authors have a conflict of interest to disclose.

References

1. D. Trajkovska, N.M. Daniloski, N. D'Cunha, A.T. Naumovski, Broache. Food Res Int. (2021). https://doi.org/10.1016/j.foodres.2020.109981
2. V.T. WeligamaThuppahige, M.A. Karim, Compr. Rev. Food Sci. Food Saf. (2022). https://doi.org/10.1111/1541-4337.12873
3. N. Tamimi, A. Mohammadi, H. Hashemi-Moghaddam, H. Baghaie, Food Sci. Nutr. (2021). https://doi.org/10.1002/fsn3.2426
4. A. Esfahani, A. Mohammadi, H. Baghaei, L. Nouri, Food Sci. Nutr. (2022). https://doi.org/10.1002/fsn3.2918
5. S. Paidari, N. Zamindar, R. Tahergorabi, M. Kargar, S. Ezzati, N. Shirani, S. Hossein, J. Food Meas. Charact. (2021). https://doi.org/10.1007/s11694-021-00979-7
6. N. Mahdavi, H. Ahari, A.A. Motallebi, S. Paidari, J. Food Meas. Charact. (2021). https://doi.org/10.1007/s11694-021-01082-7

7. S. Berti, R.J. Jagus, S.K. Flores, Food Bioprocess. Technol. (2021). https://doi.org/10.1007/s11947-021-02669-0
8. M. Mohammadi, R. Yekta, H. Hosseini, F. Shahraz, S. Hosseini, S. Shojaee-Aliabadi, A. Mohammadi, J. Food Meas. Charact. (2023). https://doi.org/10.1007/s11694-022-01509-9
9. R. Liang, S. Xu, C. Shoemaker, Y. Li, F. Zhong, Q. Huang, J. Agric. Food Chem. (2012). https://doi.org/10.1021/jf301129k
10. E.K. Silva, M.T. Gomes, M.D. Hubinger, R. Lopes Cunha, M.A.A. Meireles, Food Hydrocolloids. (2015). https://doi.org/10.1016/j.foodhyd.2015.01.001
11. K. Sharma, A. Babaei, K. Oberoi, K. Aayush, R. Sharma, S. Sharma, Bioprocess Technol. (2022). https://doi.org/10.1007/s11947-022-02811-6
12. R. Herrera Brandelero, F. Yamashita, M.V. Eiras Grossman, Carbohydr. Polym. (2010). https://doi.org/10.1016/j.carbpol.2010.06.034
13. A.G. Souza, R.R. Ferreira, L.C. Paula, S.K. Mitra, D.S. Rosa, Food Packag. Shelf Life (2021). https://doi.org/10.1016/j.fpsl.2020.100615
14. P. Alzate, S. Miramont, S. Flores, L. Gerschenson, Starch/Stärke (2017). https://doi.org/10.1002/star.201600261
15. M.B. Vásconez, S. Flores, C. Campos, J. Alvarado, L. Gerschenson, Food Res. Int. (2009). https://doi.org/10.1016/j.foodres.2009.02.026
16. S. Abbas, K. Hayat, E. Karangwa, M. Bashari, X. Zhang, Food Eng. Rev. (2013). https://doi.org/10.1007/s12393-013-9066-3
17. P. Singh, G. Kaur, A. Singh, P. Kaur, J. Food Meas. Charact. (2023). https://doi.org/10.1007/s11694-022-01635-4
18. P. Alzate, L. Gerschenson, S. Flores, Carbohydr. Polym. (2020). https://doi.org/10.1016/j.carbpol.2020.116759
19. A. Hashtjin, S. Abbasi, Food Hydrocolloids (2015). https://doi.org/10.1016/j.foodhyd.2014.08.017
20. V. Xu, J. Yang, S. Hua, Y. Hong, Z. Gu, L. Cheng, Z. Li, C. Li, Trends Food Sci. Technol. (2020). https://doi.org/10.1016/j.tifs.2020.09.026
21. K. Silva, E. Azevedo, V.M. Cunha, R.L. Hubinger, M.D. Meireles, Food Hydrocolloids (2016). https://doi.org/10.1016/j.foodhyd.2015.12.006
22. B. Saberi, S. Chockchaisawasdee, J. Golding, C. Scarlett, C. Stathopoulos, Food Hydrocolloids (2017). https://doi.org/10.1016/j.foodhyd.2017.05.042
23. R. Ortega-Toro, A. Jiménez, P. Talens, A. Chiralt, Food Hydrocolloids (2014). https://doi.org/10.1016/j.foodhyd.2013.11.011
24. S. Santacruz, C. Rivadeneira, M. Castro, Food Hydrocolloids (2015). https://doi.org/10.1016/j.foodhyd.2015.03.019
25. A. Sanchez, E. Alegria, H. Bermeo, Y. Bohorquez, H. Villada, L. Daza, C. Valenzuela, J. Food Meas. Charact. (2022). https://doi.org/10.1007/s11694-022-01491-2
26. D. Kilinc, B. Ocak, Ö. Özdestan-Ocak, J. Food Meas. Charact. (2021). https://doi.org/10.1007/s11694-020-00683-y
27. J. Prakash Maran, V. Sivakumar, K. Thirugnanasambandham, R. Sridhar, Int. J. Biol. Macromol. (2013). https://doi.org/10.1016/j.ijbiomac.2013.06.029
28. S. Hosseini, M. Rezaei, M. Zandi, F. Farahmandghavi, Ind. Crops Prod. (2015). https://doi.org/10.1016/j.indcrop.2015.01.062
29. X. Song, G. Zuoa, F. Chena, Int. J. Biol. Macromol. (2018). https://doi.org/10.1016/j.ijbiomac.2017.09.114
30. T.L. Cao, K.B. Song, Food Hydrocolloids (2019). https://doi.org/10.1016/j.foodhyd.2019.105198
31. Y. Wang, J. Luo, X. Hou, H. Wu, Q. Li, S. Li, Q. Luo, M. Li, X. Liu, G. Shen, A. Cheng, Z. Zhang, LWT Food Sci Technol. (2022). https://doi.org/10.1016/j.lwt.2022.113392
32. C.K. Nielsen, J. Kjems, T. Mygind, T. Snabe, R.L. Meyer, Front. Microbiol. (2016). https://doi.org/10.3389/fmicb.2016.01878